ON THE RECRYSTALLIZATION AND TEXTURE OF FE-36%NI ALLOY AFTER ACCUMULATIVE ROLL BONDING AND ANNEALING AT 600 °C

Kamel Tirsatine[1,*], Hiba Azzeddine[1,2], Thierry Baudin[3], Anne-Laure Helbert[3], François Brisset[3], Djamel Bradai[1]

[1] Faculté de Physique, Université des Sciences et de la Technologie Houari Boumediene, Bab Ezzouar, BP32, El Alia, Alger, Algérie.
[2] Département de physique, Faculté des sciences, Université Mohamed Boudiaf, M'Sila, Algérie.
[3] ICMMO, Université Paris-Sud, Université Paris-Saclay, UMR CNRS 8182, 91405 Orsay Cedex, France.
[*]corresponding author: e-mail: ktirsatine7@yahoo.fr

Resume
Microstructure and texture evolution of Fe-36%Ni (wt. %) alloy after 1, 5 and 10 accumulative roll-bonding (ARB) cycles and annealing at 600 °C up to 3600 seconds were studied using electron backscatter diffraction. Microstructural and textural changes after ARB and annealing were compared to those existing in the literature after conventional rolling. The microstructure was not stable at 600 °C for all ARB samples even after 3600 seconds of annealing. The recrystallization texture was dominated by the Cube {001}<100> texture component. Recrystallization kinetics were determined using microhardness measurement and were close to those after cold rolling with Avrami time exponent around unity. The texture evolution at high strain was discussed in terms of grain boundary migration obstruction by the formation of layer interfaces and small recrystallized grains near the bonded interfaces.

Available online: http://fstroj.uniza.sk/journal-mi/PDF/2017/07-2017.pdf

Article info
Article history:
Received 24 October 2016
Accepted 19 June 2017
Online 05 December 2017

Keywords:
Invar;
Accumulative roll bonding;
Recrystallization kinetics;
Ultrafine grains;
Texture;
Microstructure.

ISSN 1335-0803 (print version)
ISSN 1338-6174 (online version)

1. Introduction

Thermo-mechanical processing of alloys is of great importance for industrial specific needs. The recrystallization microstructure, texture, nature and geometry of grain boundaries are key factors influencing the mechanical properties of materials. The understanding of recrystallization kinetics and texture evolution during severe plastic deformation, especially Accumulative Roll Bonding (ARB), allows the possibility to ensure optimal conditions during thermo-mechanical processing of alloys.

Ultrafine-grained metals or alloys have demonstrated a higher combination of strength and ductility than the coarse-grained ones [1]. After ARB processing, Fe-36%Ni (wt. %) alloy samples were strengthened up to 200 % relatively to the non-deformed initial state and exhibited an ultrafine microstructure with grains having elongated shape in the rolling direction [2, 3].

Despite the numerous papers dealing with microstructure and texture evolution analysis of Fe-36%Ni alloy after conventional rolling and recrystallization annealing [4 – 8], there is a lack of knowledge on the thermal stability of the ultrafine grained Fe-36%Ni (wt.%) alloy severely deformed by ARB. In this paper we present the detailed results of electron backscatter diffraction (EBSD) measurement on the evolution of the microstructure texture as well as recrystallization kinetics of the Fe-36%Ni (wt. %) alloy processed by ARB and annealed at 600 °C.

2. Experimental procedure

The fully recrystallized Fe-36%Ni (wt. %) alloy was kindly provided by APERAM

alloys society, France. The ARB processing was carried out at 550 °C to 1, 5 and 10 cycles. The results of deformation texture and microstructure of the as deformed state were published by Tirsatine et al. [2]. Sheets of 1 mm thickness were cut from the ARBed samples and subsequently isothermally annealed at 600°C for 120, 600, and 3600 sec under H2 flux protection. The annealing temperature was selected by taking into account the results of [5].

Microstructure and microtexture was characterized using a FEG-SEM SUPRA 55 VP scanning electron microscope operating at 20 kV with the TSL Orientation Imaging Microscopy, OIMTM software. The samples were mechanically polished and then electro-polished for EBSD measurements. EBSD maps were recorded on 100 × 100 μm zones on the RD–ND (rolling and normal directions) plane of the annealed samples with a step size of 0.1 mm. The grain size data were obtained using a grain tolerance angle of 5° and the minimum grain size was chosen to be 2 pixels.

Quantitative texture analysis was carried out by calculating the Orientation Distribution Function (ODF) using the "Harmonic Method" implemented in the MTex software [9].

The micro-hardness of the specimens was measured with a Vickers microhardness tester SHIMADZU type HMV-2 using a load of 0.05 kg (HV0.05). Five hardness indentations were performed in the central area of the samples.

3. Results and discussion

3.1 Microstructure evolution after annealing of ARBed Fe-36%Ni alloy

Fig. 1 shows the orientation imaging micrographs (OIM) of Fe-36%Ni (wt. %) alloy samples after ARB processing to 1, 5 and 10 cycles and annealing at 600 °C for 120, 600 and 3600 sec. As reported earlier [2], the severely deformed microstructure of Fe-36%Ni (wt. %) alloy was characterized by elongated ultrafine grains. The grains underwent a strong refinement (down to 0.5 and 0.2 μm for length along RD and thickness along ND respectively) after 10 ARB cycles [2]. As can be seen from Fig. 1, a substantial evolution of the microstructure is noticed during annealing. The OIM of 1 ARB sample show a color gradients inside some grains which indicates that the recrystallization is not complete after annealing for 3600 sec. Contrarily, the evolution of the microstructure for 5 and 10 ARB samples looks similar and is associated to the apparition of massive and progressive recrystallization and subsequent grain growth.

Fig. 1 shows that the microstructural change during the annealing is similar to that reported in ARBed pure Cu that was associated with a typical discontinuous recrystallization mechanism [10] (Figs. 1e and f). Indeed, annealing process of pure Cu that is known to have a low stacking fault energy is different from that of materials with high stacking fault energy that are categorized as "recovery-type" [10]. Zaefferer et al. [5] reported that, Fe-36%Ni (wt. %) alloy has a relative stacking fault energy in between those of Cu and Al $\gamma rela(Cu):\gamma rela(FeNi):\gamma rela(Al)=1:3:7$, $\gamma rela=\gamma/Gb$ (γ, stacking fault energy; G, shear modulus and b length of the Burgers vector). The authors showed a deformation and recrystallization texture behavior similar to that of pure Cu. Moreover, this alloy recovers very little during cold rolling (dynamic recovery) owing to its high melting temperature and high concentration of Ni.

In the peculiar zones shown by inserts in Figs. 1j-l, a spread of small grains all over the bonded interface between layers is clearly seen. The black colored areas (non-indexed points) in the inserts of Figs. 1j, k and l correspond to holes at the mid-thickness interface obtained after the last ARB cycle (Figs. 1a, d and g).

The presence of clustered small grains

near the bonding can be associated with the shear strain induced at the sheet surfaces, in contact with the rolls, at the cycle before the last one or can be due to the wire-brushing. In both cases, this strain induces a strong germination rate that results in a so small grain size. Takata et al. [10] have already mentioned that the presence of fine grains in the bonded interface was due to the redundant shear deformation or/and wire-brushing. In our case, we used a lubricated ARB process that probably limited shear strain, and it can be supposed that the fine grains, in the bonding area, are mainly due to the wire-brushing.

After 10 ARB cycles, the strip thickness is around 0.97 μm. The mean grain size measured by the line-intercept method is around 10 μm. This result shows clearly that a good bonding is achieved and the grains can cross the layer boundaries and grow all over the layer thickness. In fact, whatever the cycle number, the low bonding quality of the mid-thickness interface inhibits the boundary migration and thus the grain growth.

Fig. 2 shows the evolution of the grain diameter of all grains as well as the recrystallized grains of Fe-36%Ni alloy after ARB processing and annealing at 600 °C up to 3600 sec. The grain size was estimated from the equivalent circle diameter. Concerning the global grain size (all grains), it is clear that the grain diameter increases significantly upon annealing after 5 and 10 ARB cycles especially after 600 sec whereas it remains quite constant after 1 ARB cycle. In this alloy, the recrystallization mechanism corresponds to a discontinuous recrystallization as it can be observed in Fig. 1. This recrystallization consists in nucleation followed by nuclei growth into the deformed matrix by Strain Induced Boundary Migration (SIBM) mechanism [10] and it leads to equiaxed grains. In the special case of 1 ARB cycle, the appearance of recrystallized grains is delayed (Fig. 1g) because of the lower energy stored during the deformation processing. The grain size of 1 ARB sample remains constant because the recrystallized grains have the same equivalent diameter than the all grains at this special recrystallization time (Fig. 2, dotted lines). In the case of 5 and 10 ARB cycles, the grain size notably increases after annealing for 600 sec. Note that after 1 ARB cycle, the microstructure is partially recrystallized after 3600 sec annealing. On the contrary, for the same annealing time, the recrystallization is complete for the two largest cycle numbers. It has already been observed in the literature that the growth rate of the grains in the fine-grained material (like in 5 and 10 ARB samples) is some times faster than that of the coarse-grained material (like in 1 ARB sample) at the same temperature. Such difference in the recrystallization kinetics could be ascribed to the stored energy during the deformation [11]. Moreover, the achieved grain diameter after annealing for 360 sec is close to the initial grain size of the unprocessed material ($8 < d < 10$ μm) [2]. Unfortunately, this ARB processing route does not maintain a refined microstructure after complete recrystallization, contrary to the ECAE processing of a Copper alloy (3 μm) [12].

Furthermore, it can be observed that the achieved grain size is slightly more important after 5 ARB cycles (11 μm) than after 10 ARB cycles (8 μm). This can be explained by the fact that after 10 ARB cycles the deformation amount is larger, thus the nucleus number is increased and, as a consequence, the final grain size is smaller.

Fig. 3 shows the evolution of the twin fraction as a function of ARB cycle number and annealing time. The increase of twin fraction is consistent with the occurrence of the discontinuous recrystallization and the associated grain growth [13]. Additionally, it is seen that twin fraction after complete recrystallization is similar (around 40 %) whatever the ARB cycle number 5 or 10.

Fig. 4 presents the evolution of high angle grain boundary (HAGB) fraction

of the Fe-36%Ni (wt. %) alloy after ARB processing and annealing at 600 °C for 120, 600 and 3600 sec. The evolution of HAGB fraction shows an increase after 1600 sec as recrystallization develops. The HAGB fraction reaches 80 % after complete recrystallization for 5 and 10 ARB samples (annealing for 3600 sec), which indicates that the alloy is not isotropic (HAGB > 95 %). The low HAGB fraction (about 40 %) for 1 ARB sample is due to the partial recrystallization of the sample.

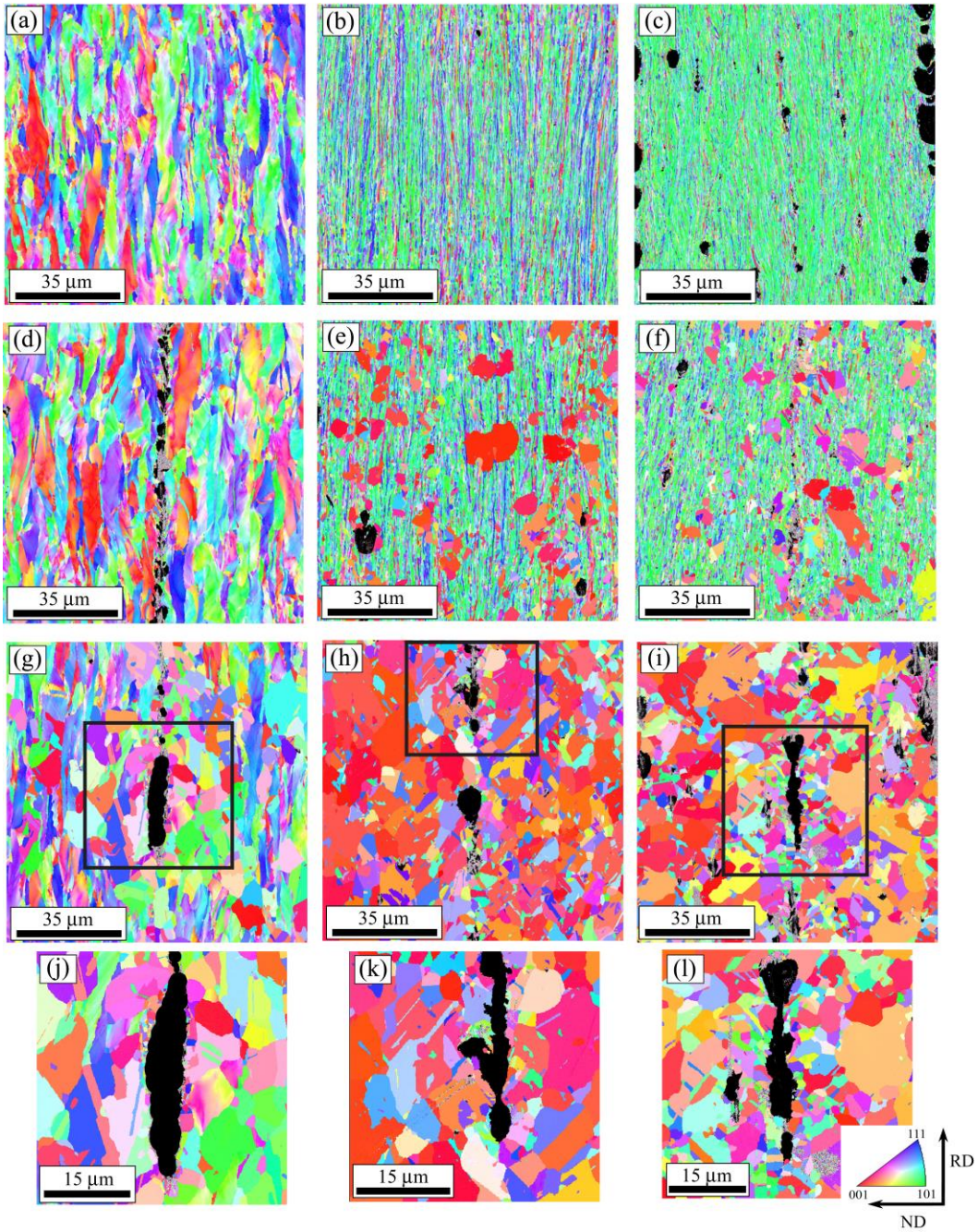

Fig. 1. OIM of Fe-36%Ni (wt. %) alloy after ARB processing to 1cycle and annealed at 600° C for (a) 120 sec, (b) 600 sec, (c) 3600 sec, 5 cycles and annealed at 600 °C for (d) 120 sec, (e) 600 sec, (f) 3600 sec and 10 cycles and annealed at 600 °C for (g) 120 sec, (h) 600 sec, (i) 3600 sec. Peculiar zones near bonding zones are shown as inserts.
(full colour version available online)

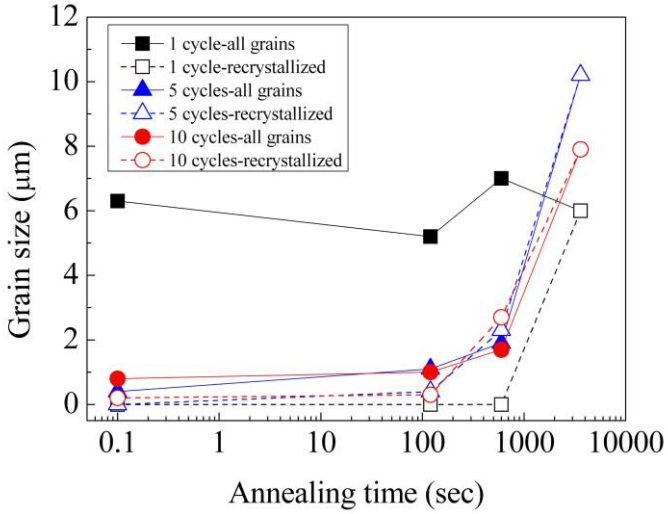

Fig. 2. Evolution of the grain diameter of all grains and the recrystallized grains of Fe-36%Ni (wt. %) alloy after ARB processing and annealing at 600 °C up to 3600 sec.
(full colour version available online)

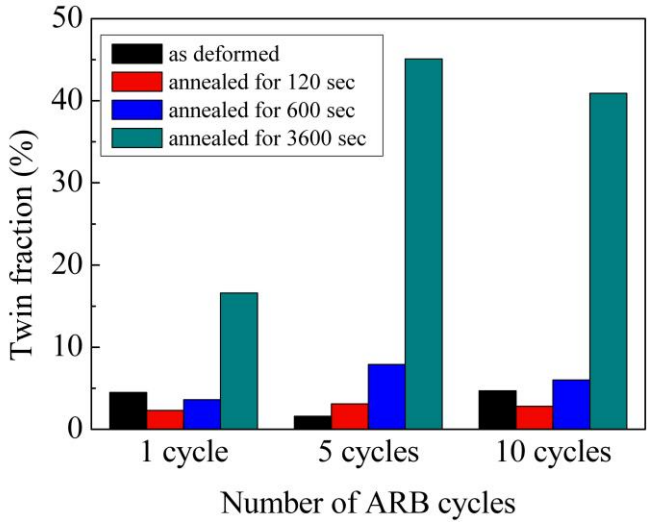

Fig. 3. Evolution of the Twin fraction as a function of ARB cycle number and annealing time.
(full colour version available online)

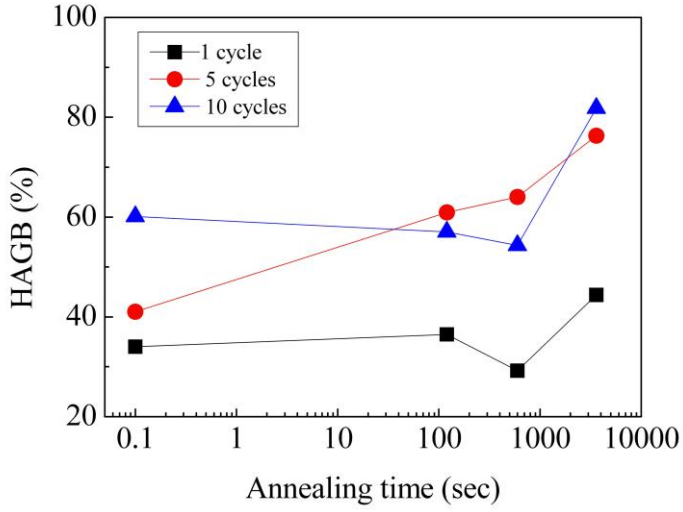

Fig. 4. Evolution of HAGB fraction of Fe-36%Ni (wt. %) alloy after ARB processing and annealing at 600 °C up to 3600 sec.
(full colour version available online)

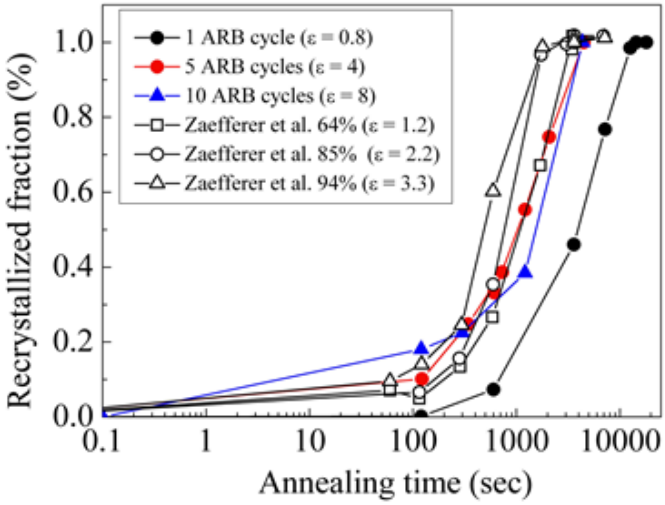

Fig.5 Recrystallized volume fraction versus annealing time of the Fe-36%Ni (wt. %) alloy after ARB processing and annealing at 600 °C. Data from Reference [5] are shown for comparison.
(full colour version available online)

Table 1
The JMAK parameters variation determined in the present study. Results from Zaefferer et al. [5] are also reported for comparison.

	n	k
1 cycle	1.65	-13.36
5 cycles	0.80	-5.33
10 cycles	0.90	-5.33
69 % [5]	1.17	-8.62
85 % [5]	1.38	-9.50
94 % [5]	1.06	-6.92

3.2 Kinetics of recrystallization during annealing of ARBed Fe-36%Ni alloy

Fig. 5 presents the recrystallized volume fraction, *X*, versus annealing time deduced from the microhardness measurements using standard equation [14] (1):

$$X(t) = \frac{Hv_{max} - Hv(t)}{Hv_{max} - Hv_{min}} \qquad (1)$$

Where $Hv(t)$ stands for hardness value at time t, Hv_{max} is the maximum hardness of the as-severely deformed sample (at $t = 0$) and Hv_{min} is the minimum hardness of the fully recrystallized sample.

Zaefferer et al. [5] have published data on the kinetics of recrystallization of the same alloy after cold rolling and annealing at 600 °C, they are plotted together for comparison. It can be clearly seen that the 5 (ε = 4) and 10 (ε = 8) ARB samples kinetics are close to the 64 % (ε = 1.2) cold-rolled sample kinetics. For only the 1 ARB sample, kinetics are slower. The recrystallization of the Fe-36%Ni (wt. %) alloy sample after 5 ARB cycles occurs lately than for the cold rolled sample despite the closest equivalent strain (95 % thickness reduction, ε = 3.45). The explanation of these findings could be associated with the processing temperature. Indeed, material stores more energy during cold rolling than during hot ARB.

It can also be observed that after 300 sec, the recrystallization in the 5 ARB sample seems to be more effective than in the 10 ARB cycles. This finding is in line with the observation made by Beck et al. [15], who found that the grain boundary migration rate

was slower in the specimen containing strips. In our case, the 10 ARB sample accumulated 1024 strips instead of 512 in the 5 ARB sample.

The kinetics of recrystallization could also be discussed using the Johnson-Mehl-Avrami-Kolmogorov (JMAK) relationship [16 – 18] (2) that gives the variation of the recrystallized fraction versus the annealing time:

$$X(t) = 1 - \exp(-kt^n) \quad (2)$$

Where X is the recrystallized fraction, t is the annealing time, k is temperature dependent and n is the Avrami time exponent. The n and k parameters can easy been obtained from the linearization of the JMAK equation. Table 1 presents the n and k values obtained for 1, 5 and 10 ARB samples. Results from Zaefferer et al. [5] are also reported in Table 1 for comparison.

It can be seen from Table 1 that the values of the Avrami time exponent n are around 1 for all samples which indicates the presence of heterogeneous site saturated nucleation of recrystallized grains [19]. The n values obtained in this study are slightly different from those calculated from data of Zaefferer et al. [5]. This difference may be due to the processing conditions that influence the kinetics of the recrystallization. Indeed, the data of Zaefferer et al. [5] were obtained for a cold rolled and annealing samples at 600 °C while in the present study, they were deduced for hot ARBed samples (at 550 °C) and annealed at 600 °C.

3.3 Texture evolution after annealing of ARBed Fe-36%Ni alloy

Fig. 6 shows the calculated ODF sections at φ2 = 0, 45 and 65° of Fe-36%Ni (wt. %) alloy after ARB processing for 1, 5, 10 cycles and annealing at 600°C for 120, 600 and 3600 sec. The location of ideal orientations is also indicated on the ODF sections. The main ideal texture components positions of FCC alloys and their descriptions are given in Table 2. As already reported by Tirsatine et al. [2], the texture of as deformed samples showed the presence of FCC dominant rolling texture components (Copper, S and Brass). Those components with a certain grain orientation distribution affect material proprieties during the thermomechanical treatment, yielding valuable information on them properties. It is worth noting that the texture of the samples after 1, 5 and 10 ARB cycles and annealing at 600 °C for 120 sec looks similar to that prior to annealing (presented in Reference [2]). With increasing annealing time, a more or less sharpening of Cube component accompanied by gradual decrease of Copper, S and Brass components are depicted. The variation of Cube fraction as function of annealing time in 1, 5 and 10 ARB samples is shown in Fig. 7.

After one hour annealing at 600 °C of 1 ARB sample, the Copper, S and Brass deformation texture components remain present. There is also a small amount of Cube retained from the initial state of the alloy (before deformation) [2]. Figs. 6 and 7 confirm indubitably that annealing of the 1 ARB cycle did not affect totally the deformation texture components that exhibited a sort of stability even after 3600 sec. At low deformation straining, the texture is retained because all the texture components may nucleate. Moreover, the texture tended to be isotropic because the twining might operate for all he texture components and hence generated new orientations. The global weakening of the texture should be ascribed to the occurrence of multiple twinning as discussed by [20]. This multiple twinning has already been observed in Al and Cu monocrystals and did not lead to a random texture but rather to a noticeable failing of the texture.

Annealing the samples after 5 and 10 ARB cycles modifies the texture components

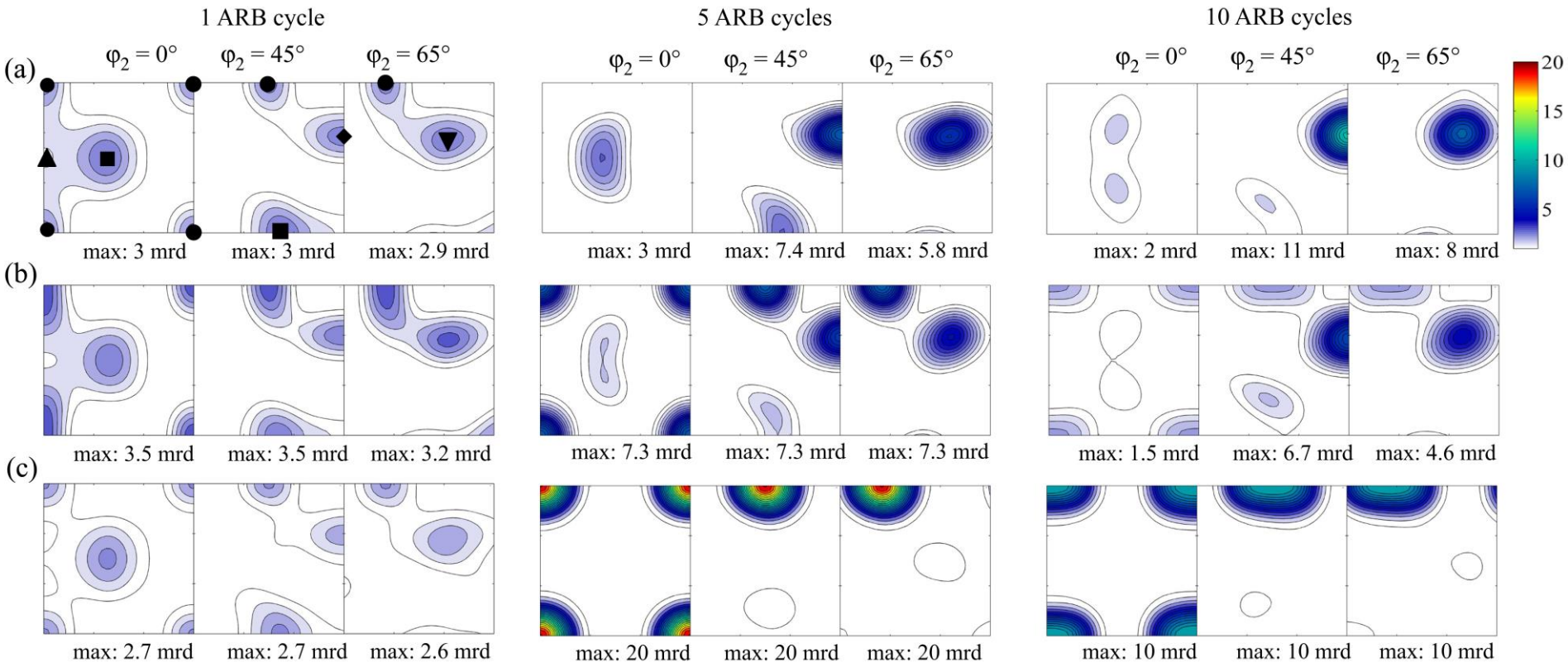

Fig. 6. ODF sections at φ2= 0, 45 and 65 ° of the Fe-36%Ni (wt. %) alloy after ARB processing and annealing at 600 °C for: (a) 120 sec, (b) 600 sec and (c) 3600 sec. (full colour version available online)

Table 2

Main ideal rolling texture components of FCC alloys.

Component		{hkl}<uvw>	Euler Angle		
			φ_1	φ	φ_2
■	Brass	{110}<112>	35°	35°	45°
▲	Goss	{110}<001>	0°	45°	0°
●	Cube	{001}<100>	0°	0°	0°
◆	Copper	{112}<111>	90°	35°	45°
▼	*S*	{231}<346>	59°	29°	63°

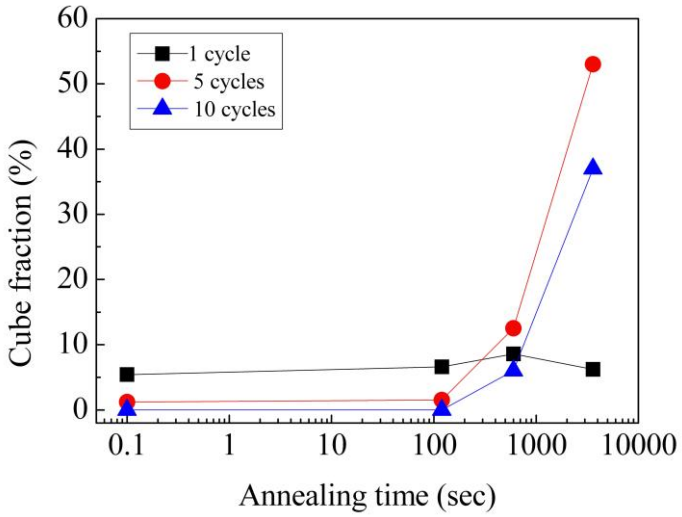

Fig. 7. Cube fraction in Fe-36%Ni (wt. %) alloy after ARB processing and annealing at 600 °C up to 3600 sec: (a) 1 ARB cycle, (b) 5 ARB cycles and (c) 10 ARB cycles.
(full colour version available online)

volume fractions and shows an overall decrease of the Copper, S, Brass deformation texture components and a net increase of the Cube component. The development of the Cube texture after conventional cold and hot deformation has been well studied in Fe-Ni system [21–23]. It is worth noting that annealing of samples after 5 and 10 ARB cycles leads to the development of a weak (with volume fraction ranging between 5 % and 2.5 %), Twin Cube (122)<221> (45°, 70.53°, 45°) component as can be seen in Fig. 6. **It is to be noted that this component did not exist in the deformed material but developed during the recrystallization annealing.**

Extensive observations by means of X-ray texture measurements and transmission electron microscopy (TEM) observations, including orientation measurement, of first stages of recrystallization were performed by [5, 20] in cold-rolled Fe-36%Ni alloy. Three deformation-induced heterogeneities that are lamella bands (LB), cube bands (CB) and shear bands (SB) were analyzed in relation to cube texture development. It has been explicitly shown that LB and SB did not play any role in recrystallization nucleation or texture formation. The CB were very appropriate for the nucleation of cube grains owing to their high orientation gradient, high misorientation across the band and well recovered cells [5, 20]. Since the texture evolution and kinetics of recrystallization of Fe-36%Ni alloy after processing by ARB (present study) and cold rolling [5, 20] are quiet close, it can be assumed that the same mechanisms of cube grain formation and evolution may operate.

After annealing for 600 sec, the Cube volume fraction in 5 ARB cycles is around 12 % but in the 10 ARB cycles it is just 6 %. This anomalous effect has already been reported

in pure Cu processed by ARB and annealed at 150 °C up to 600 min [10]. These authors have reported the existence of large amount of small recrystallized grains formed around the bonded interfaces and having several different orientations (similar observations are reported in Fig. 1). These small grains were considered hence as principal weakening factor of the Cube texture development. These interfaces were previously wire-brushed which can induce a local area of severe plastic deformation, an origin of submicronic grain creation as for example in SMATed alloys [24]. These small grains contain low energy and have the same probability as Cube grains to nucleate. As the interface number increases, from 5 to 10 ARB cycles, the random nucleation increases and leads to a decrease of the Cube fraction. This texture dispersion can be verified during the first step of recrystallization (600 sec) and persists up to the final recrystallization (50 % and 35 % Cube fraction for 5 and 10 ARB cycles respectively).

To sum up, the ARB process does not allow developing a sharp Cube texture contrarily to what was obtained after high cold-rolling and annealing knowing that this sharp texture is often desired for superconductor applications [25]. An attempt to perform the ARB process at lower temperatures could permit increasing this Cube fraction. It remains to be checked whether a lower temperature could limit the grain growth. Moreover, it could be interesting to increase the ARB cycle number to increase the severe plastic deformation and then the nuclei number, in order to decrease the grain size after complete recrystallization.

4. Conclusion

The microstructure and texture of Fe-36%Ni (wt.%) alloy severely deformed by ARB up to 10 cycles and annealed at 600 °C up 3600 sec has been investigated using EBSD, the main results are summarized below:

- The microstructure of Fe-36%Ni (wt.%) alloy was not stable during annealing at 600°C.
- The recrystallization kinetics and texture after Accumulative Roll Bonding were similar to those after conventional cold rolling. The Cube texture component dominated but with weaker intensity and volume fraction.
- The recrystallization kinetics was expressed by the Avrami time exponent around 1 for all samples. This value indicates heterogeneous site saturated nucleation of recrystallized grains.
- The decrease in Cube fraction between 5 and 10 ARB cycles was probably due to the presence of small grains at the wire-brushed interfaces induced by severe plastic deformation.

Acknowledgements

The authors wish to thank Pierre-Louis REYDET from APERAM-alloys Imphy Society, France, for kindly providing the Fe-36%Ni (wt. %) alloy. This work was supported in part by the TASSILI program No. 12MDU862 / EGIDE: 26481WM.

References

[1] A. Azushima, R. Kopp, A. Korhonen, D.Y. Yang, F. Micari, G.D. Lahoti, P. Groche, J. Yanagimoto, N. Tsuji, A. Rosochowski, A. Yanagida CIRP: Annals-Manufacturing Technology 57 (2008) 716–735.

[2] K. Tirsatine, H. Azzeddine, T. Baudin, A.L. Helbert, F. Brisset, B. Alili, D. Bradai: J. Alloys Compd. 610 (2014) 352–360.

[3] N. Kamikawa, T. Sakai, N. Tsuji: Acta Materialia 55(17) (2007) 5873–5888.

[4] N. Tsuji, H. Takebayashi, T. Takiguehi, K. Tsuzaki, T. Maki: Acta Metall. Mater. 43 (1995)743–754.

[5] S. Zaefferer, T. Baudin, R. Pennelle: Acta mater. 49(6) (2001) 1105–1122.

[6] S. Chhann, D. Solas, A.L. Etter, R. Pennelle,

T. Baudin: Mater. Sci. Forum 550 (2007) 551-556.

[7] N. Tsuji, H. Takebayashi, T. Takiguchi, K. Tsuzaki and T. Maki: Acta Metallurgica et Materialia, 43 (1995) 755–768.

[8] B.L. Li, N. Tsuji, N. Kamikawa: Mater. Sci. Eng. A 423(1-2) (2006) 331–342.

[9] F. Bachmann, R. Hielscher, H. Schaeben: Solid. State. Phenom. 160 (2010) 63–68.

[10] N. Takata, K. Yamada, K. Ikeda, F. Yoshida, H. Nakashima, N. Tsuji: Mater. Trans. 48(8) (2007) 2043–2048.

[11] M. Cieslar, M. Poková: Materials 7 (2014) 8058–8069.

[12] Z. Guo, D. Solas, A.L. Etter, T. Baudin, R. Penelle: Mater. Sci. Forum 426–432 (2003) 2723–2728.

[13] W. Wang, F. Brisset, A.L. Helbert, D. Solas, I. Drouelle, M.H. Mathon, T. Baudin: Mater. Sci. Eng. A, 589 (2014) 112–118.

[14] O. R. Myhr, O.Grong: Acta Metall. Mater. 39(11) (1991) 2693–2702.

[15] P.A. Beck, J.C. Kremer, L.J. Demer: Transaction of American Institute of Mining, Metallurgical, and Petroleum Engineers 175 (1948) 372.

[16] A.N. Kolmogorov: Akad. Nauk. USSR Izv. Ser. Mat. 1(3) (1937) 355–359.

[17] W.A. Johnson, R.F. Mehl: Trans. Metall. Soc. AIME 135 (1939) 416–458.

[18] M. Avrami: J. Chem. Phys. 7 (1939) 1103–1112.

[19] J.W. Christian: The Theory of Transformations in Metals and Alloys: Advanced Textbook in Physical Metallurgy, second ed., Peramon Press, Oxford, 1975.

[20] F. Julliard: Study of Recrystallization Mechanisms in Invar alloy, Ph.D Thesis, Université Paris Sud, Orsay, France (2001).

[21] R. Penelle, T. Baudin: Adv. Eng. Mater. 12(10) (2010) 1047–1052.

[22] V. Branger, M. H. Mathon, T. Baudin, R. Penelle: Scripta Mater. 43(4) (2000) 325–330.

[23] F. Caleyo, T. Baudin, R. Penelle, V. Venegas: Scripta Mater. 45(4) (2001) 413–420.

[24] G. Proust, D. Retraint, M. Chemkhi, A. Roos, C. Demangel: Microsc Microanal 21(4) (2015) 919–926.

[25] Y. Ateba Betanda, A.L. Helbert, F. Brisset, M. Wehbi, M.H. Mathon, T. Waeckerlé, T. Baudin: Adv. Eng. Mater. 16(7) (2014) 933–939.